

Figure S1 A Phase diagram of DS2 circuit in configuration #6.1 for which the suppression parameter $b_{21} = 0.5$ placing the dynamics beyond a saddle-node bifurcation leading to the loss of one fixed point. Configuration #6.1 is similar to #9 except that $b_{21} = 0.5$. The global fixed points of the dynamics (#1 saddle node, #2 stable node and #3 stable node) are located at the intersections of all three null-surfaces. The red, black and green elongated “clouds” of dots are numerical constructs to assist in locating the intersections of any two null-surfaces (“bi-null-surface intersections”). B Same as A, except null-surfaces are removed for clarity. The global fixed points of the dynamics are located at the intersections of the bi-null-surface intersection locator “clouds”. The fixed point locations, eigenvalues and stability assignments are given in Supplementary Table 8.

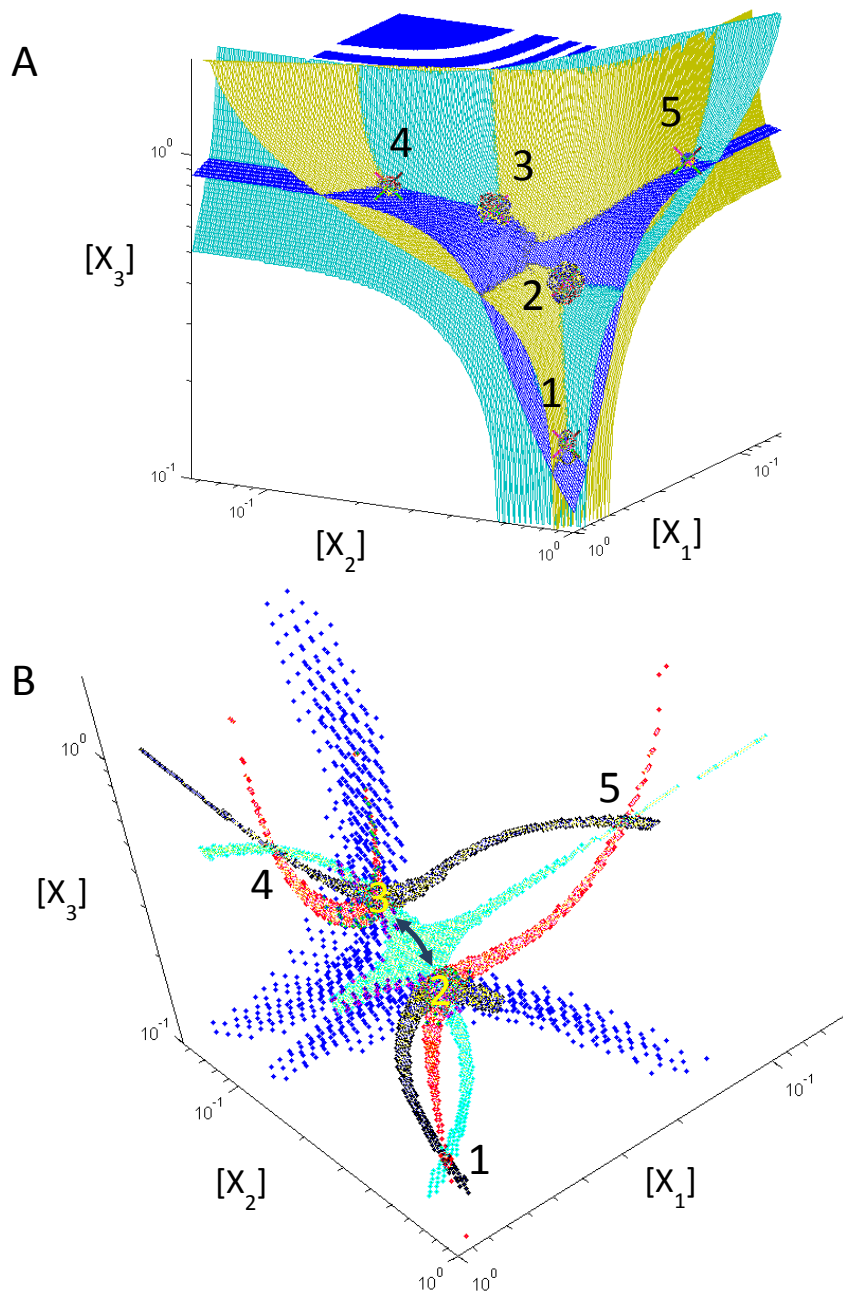


Figure S2 A Phase diagram of DS2 circuit in configuration #9 for which the suppression parameter $b_{21} = 0.85$. The circuit dynamical regime is in a region where five fixed points co-exist. B Phase diagram with null-surfaces removed. The viewpoint is slightly altered for visibility. The bi-surface intersection clouds explain the birth of the two saddles (#2 and #3, in yellow). The two-headed arrow shows how increasing “ b_{21} ” results in splitting off originally one saddle (at $b_{21} = 0.5$) into here two (at $b_{21}=0.85$). Fixed points #1, #4 and #5 are stable fixed points. Global dynamical fixed points of any type always occur at the intersection of bi-null-surface intersection “clouds”. The generalized 3D two-leaved null-surface is shown in blue. The fixed point locations, eigenvalues and stability assignments are given in Supplementary Table 9.

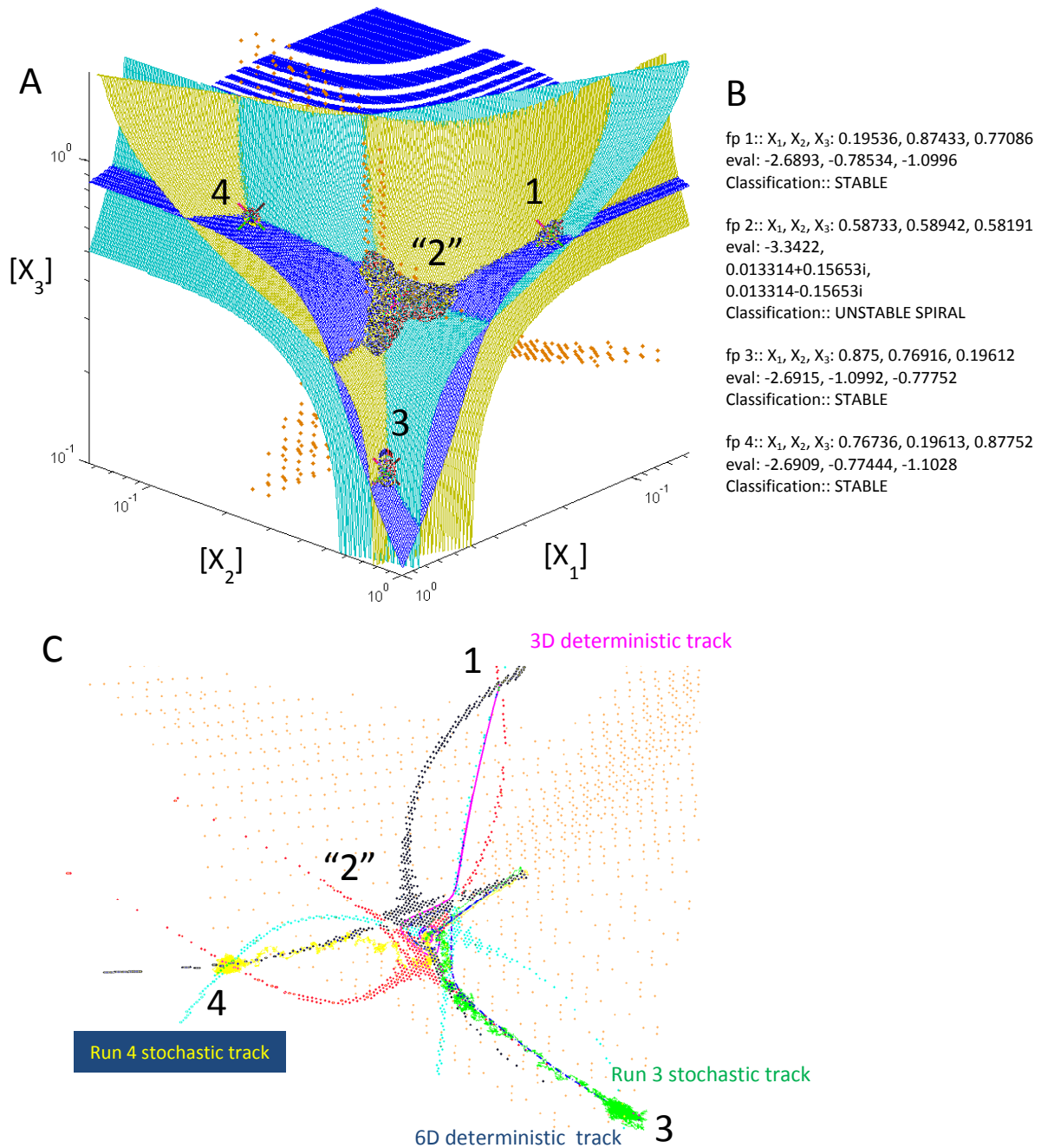


Figure S3 Phase diagram of the 3D DS2 circuit in parameter set 12 ($b_{\text{common}}=0.85$). Here, timescale separation is not enforced. B Fixed point locations, eigenvalues and stabilities. There are three stable fixed points, #1, #3 and #4. The stability of "2" is discussed in the text. The clouds of black dots numerically approximate the location of the fixed points. The generalized separatrix surface (shown in red) is visible in the background. C Expanded view showing deterministic and stochastic simulations revealing the effect of timescale separation. Details in the text.

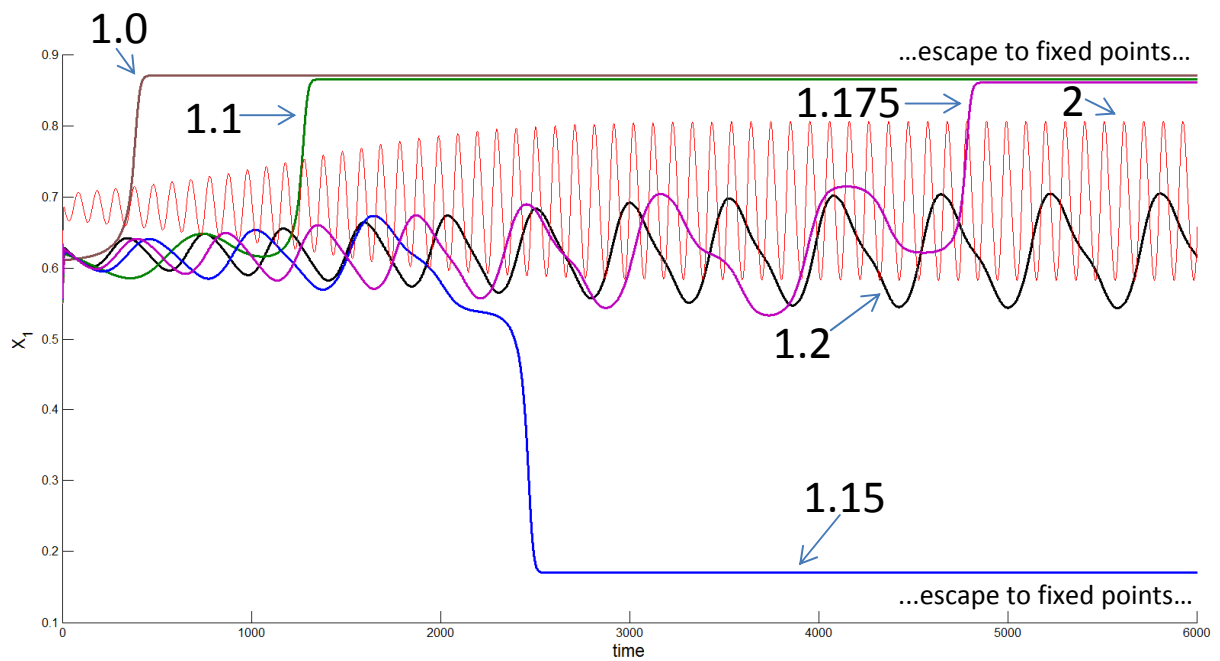


Figure S4 Several deterministic tracks in DS2, 6D (parameterization #12.1) with “bcommon” varied as shown. The y-axis shows X_1 . The x-axis shows time. Between bcommon=1.175 and 1.2, the dynamical regime switches from “escape to fixed points” (top and bottom plateaus), to oscillations (middle region). The origin of all the tracks is $[X_1, X_2, X_3, \text{mRNAX}_1, \text{mRNAX}_2, \text{mRNAX}_3] = [.63406 \ 0.62865 \ 0.60653 \ .0100 \ .0100 \ .0100]$.

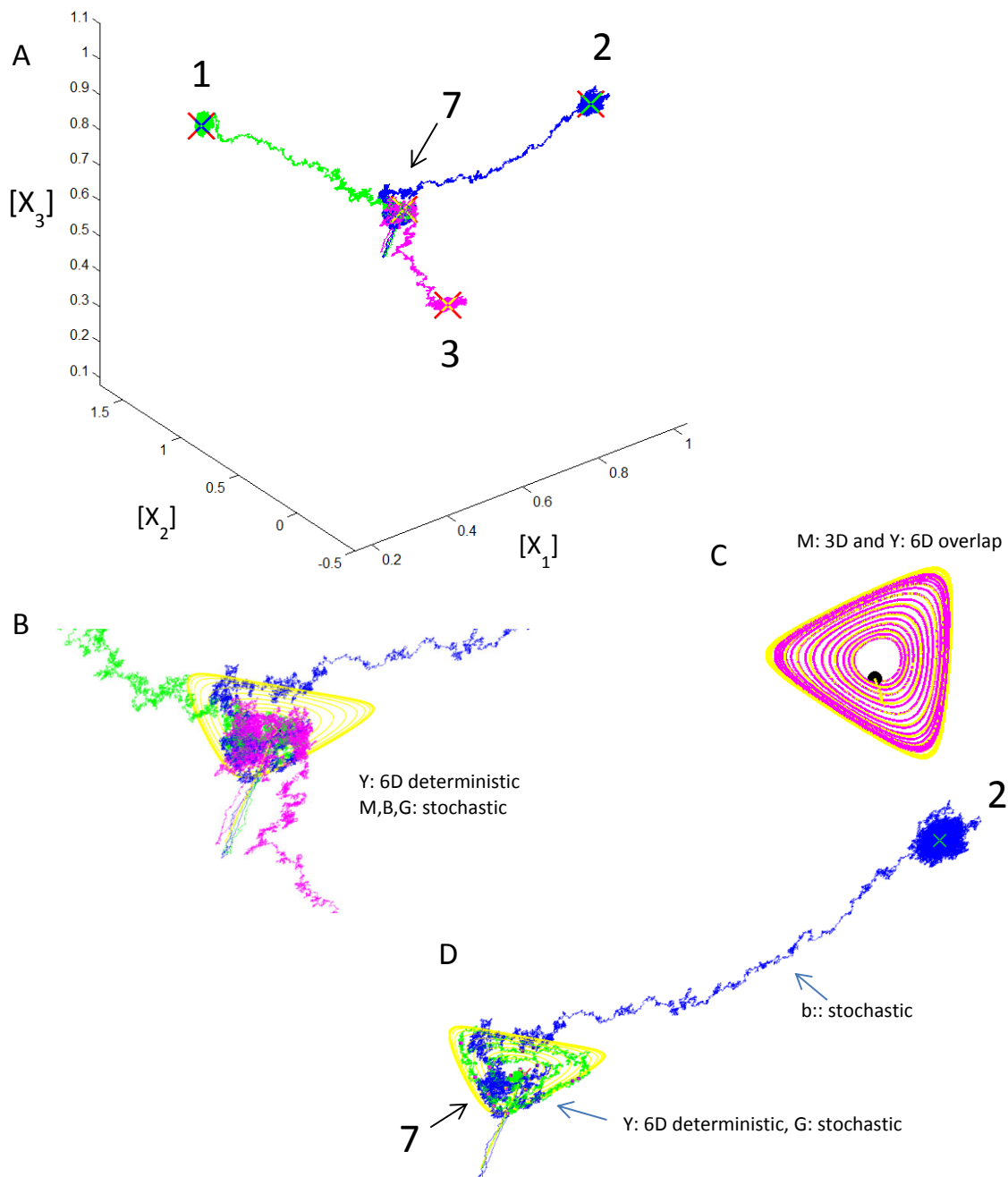


Figure S5 A DS2 circuit in configuration #15 for which $b_{\text{common}}=1.2$ but otherwise similar to #12.1, hence with high time-scale separation. Here, the null-surfaces are removed for clarity. Three stochastic tracks with different seeds all originating from fixed point #7 (arrow) reach each of the three stable fixed points, #1,#2 and #3. B Details of the stochastic wandering in the vicinity of the saddles (#4, #5 and #6 omitted for clarity). The yellow track is a 6D deterministic track. C Agreement of 6D (yellow) and 3D (magenta) tracks. At $b_{\text{common}}=1.2$, there is an orbit both in 6D and in 3D. D The blue stochastic track escapes to fixed point #2. However, the green stochastic track with $10^{1/2}$ less intrinsic noise does not. As expected, it more closely agrees with its deterministic 6D counterpart (yellow).

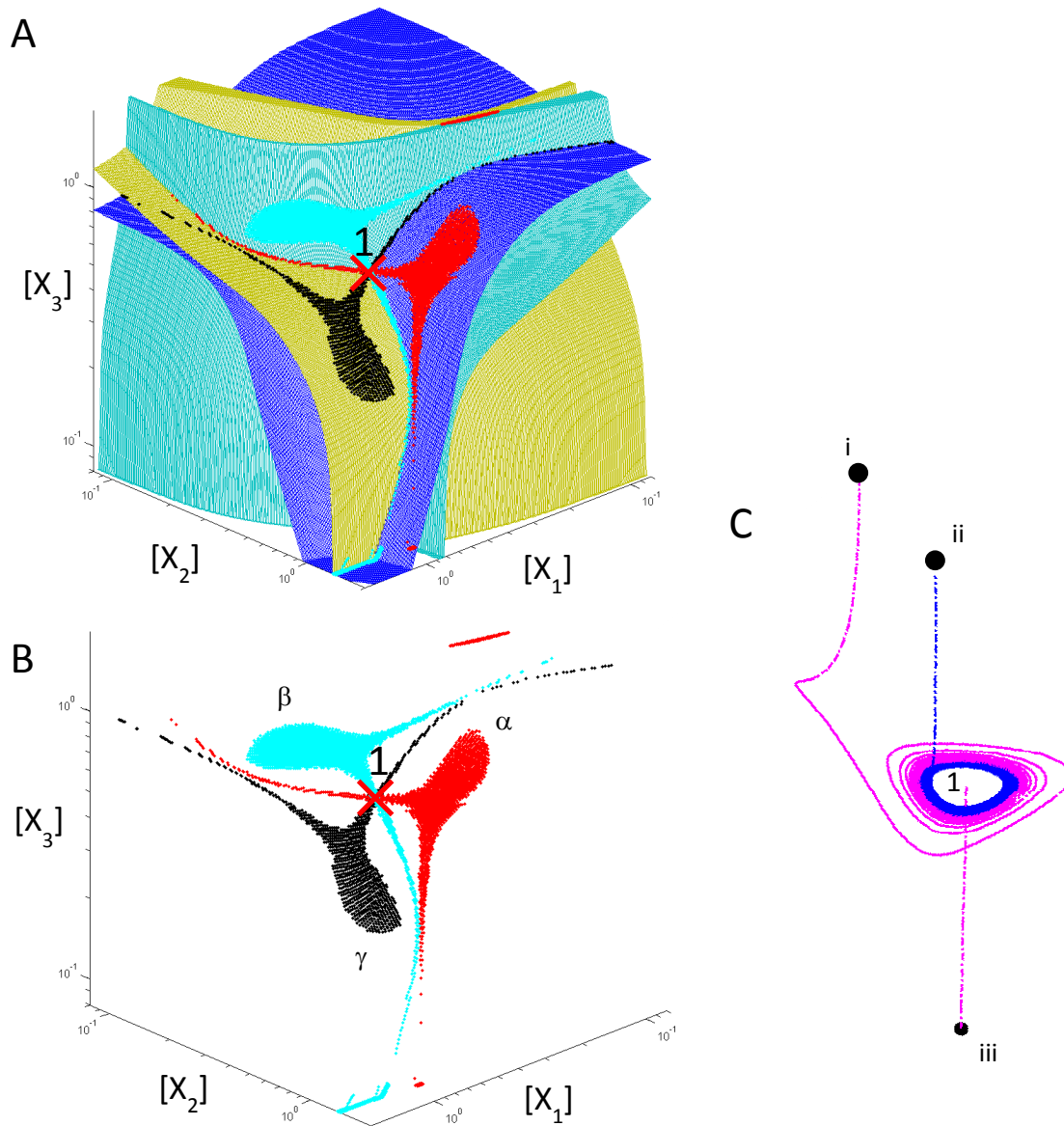


Figure S6 A DS2 circuit in configuration #20 for which $b_{\text{common}}=2.0$ but otherwise similar to #12.1, hence with high time-scale separation. A With null-surfaces. B Without null-surfaces, for better visibility. The three elongated clouds of locator points along the bi-null-surface intersections are shown in red, black and green. The flat remnants of the saddle areas are clearly visible near locations α , β and γ . The only global fixed point of the dynamics is indicated by a cross and is labeled with “1” (stable spiral). C Three 6 D trajectories started from the given locations: i) falling into a limit cycle from outside ii) falling into the same limit cycle but from inside and iii) falling into the stable fixed point only when the track is started directly on the first eigenvector direction. See text for discussion of the stability of this fixed point. The single fixed point location, eigenvalue and stability assignment is in Supplementary Table 10.

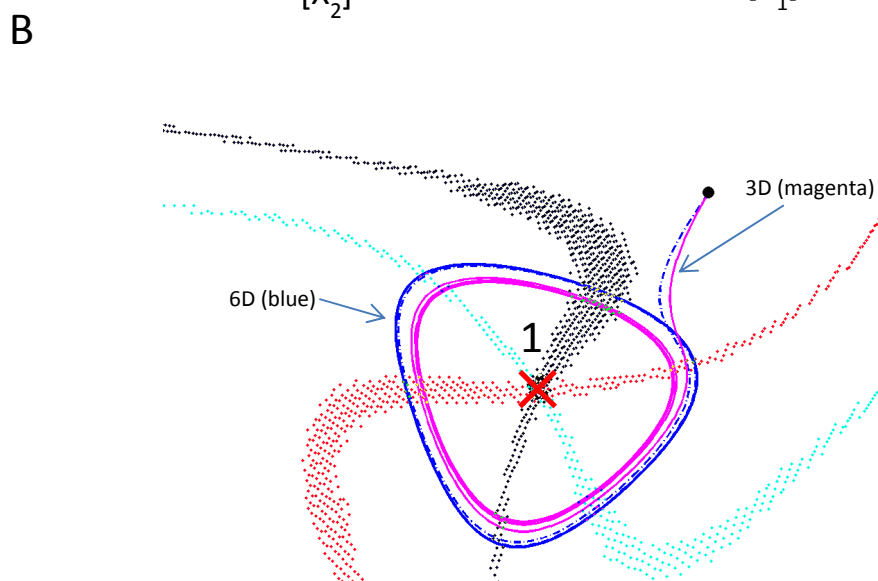
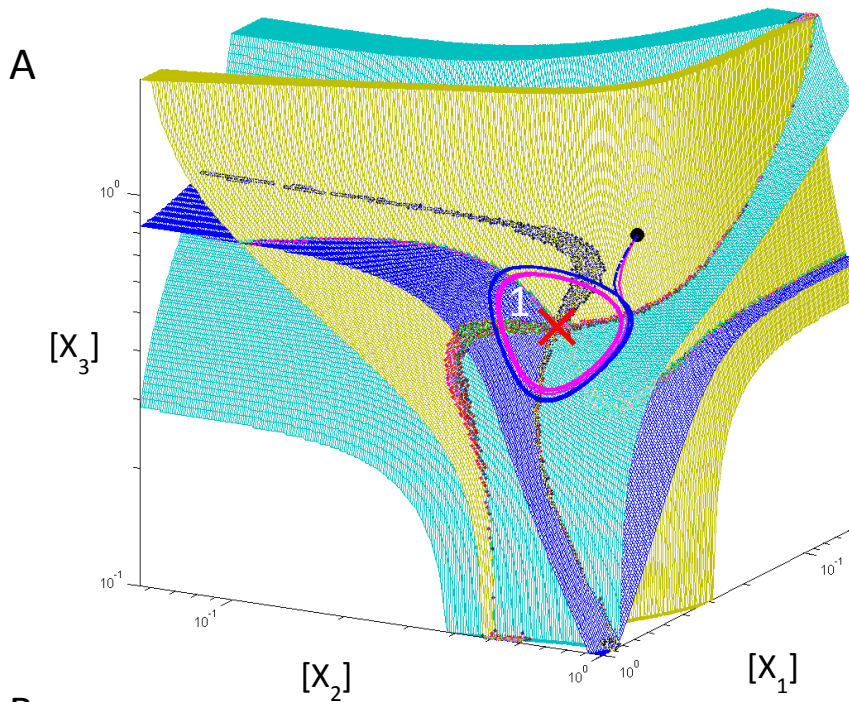


Figure S7 A DS2 circuit in configuration #16 for which $b_{\text{common}}=0.5$ but otherwise similar to #12.1, hence with high time-scale separation. Both 3D and 6D bifurcation analyses predict only one unstable fixed point located at the intersection of the bi-null-surface “clouds” of locator points. Surrounding this fixed point is a large stable orbit. One 3D and one 6D track originate at the black dot and plunge towards the stable orbit. B Details of the 3D and 6D trajectories with the null-surfaces removed. As expected, there is high agreement between 3D and 6D tracks since the timescale separation in 6D is large.

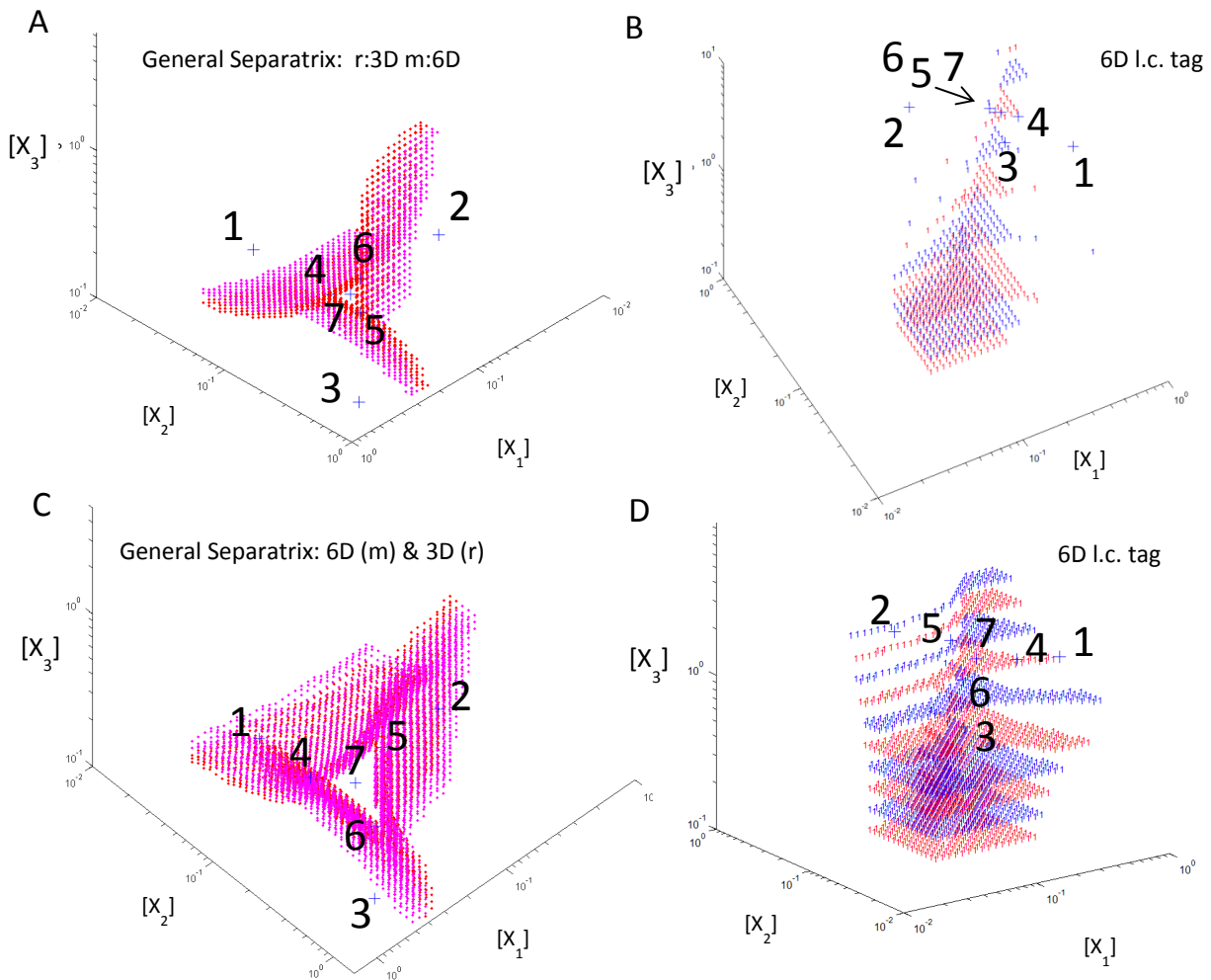


Figure S8 Computation of the location of the generalized separatrix surfaces in the DS2 circuit. Panel A and B, $b_{\text{common}}=1.2$ Panel C and D, $b_{\text{common}}=1.5$. Panel A shows an overlay of the 3D (red) and the 6D (purple) surfaces. The computation was performed using configuration #24 (reference time-scale separation) at $b_{\text{common}}=1.2$, in the dynamical region where rotation coexists with attractive fixed points of the dynamics. Panel B shows the loci of all initial conditions tagged as leading to the dynamic attractor (limit cycle, l.c.), in 6D. Colors red and blue alternate along X_3 levels to provide improved visibility. The equivalent 3D graph is omitted; it is similar but slightly smaller in X_1 , X_2 extent at each X_3 level. C 6D (magenta) and 3D (red) general separatrix surfaces are overlapped. The computation was performed using parameter configuration #24.1 (reference time-scale separation, similar to 12.1 except that $b_{\text{common}}=1.5$). Fixed points 1, 2 and 3 are stable nodes; 4, 5 and 6 are saddle nodes, and 7 is a stable spiral in 3D. In 6D, at this value of parameter asymmetry, the dynamics exhibits a limit cycle. In 3D, for which time-scale separation is infinite by construction, there is no limit cycle.

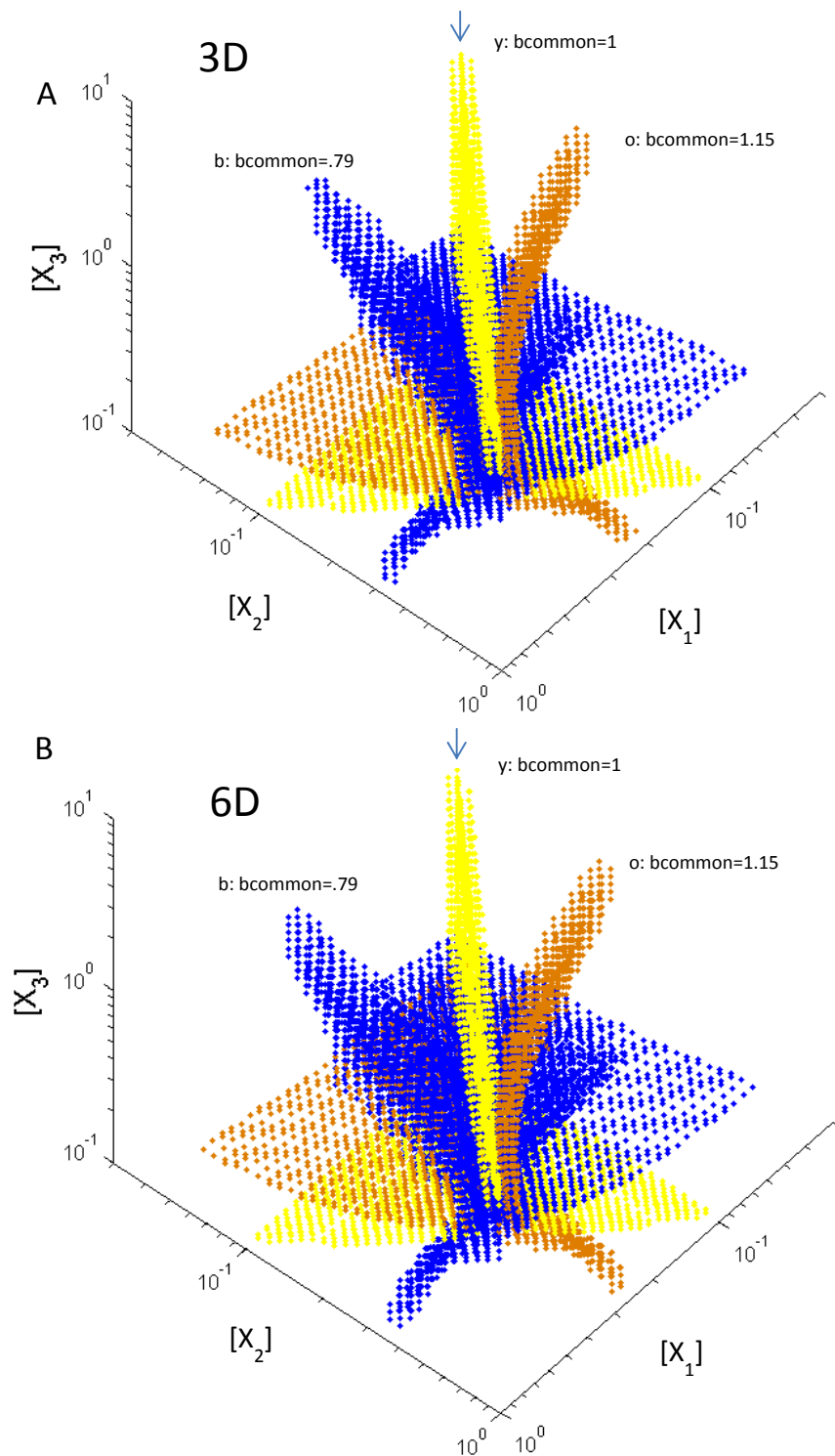


Figure S9 Overlay of the generalized separatrix surfaces at three values of “bcommon”, for 3D (Panel A) and 6D (Panel B) DS2. These values of “bcommon” span the range over which the system presents no l.c. In the symmetric case, the middle pane of each of the tree leaves is the attractive manifold of the center saddle (arrows). In the asymmetric cases, the central fixed point is an unstable spiral. Configurations #12.5, #12.6 and #12.7 are similar to #12.1 except for $b_{\text{common}}=1$, 1.15 and 0.79, respectively.

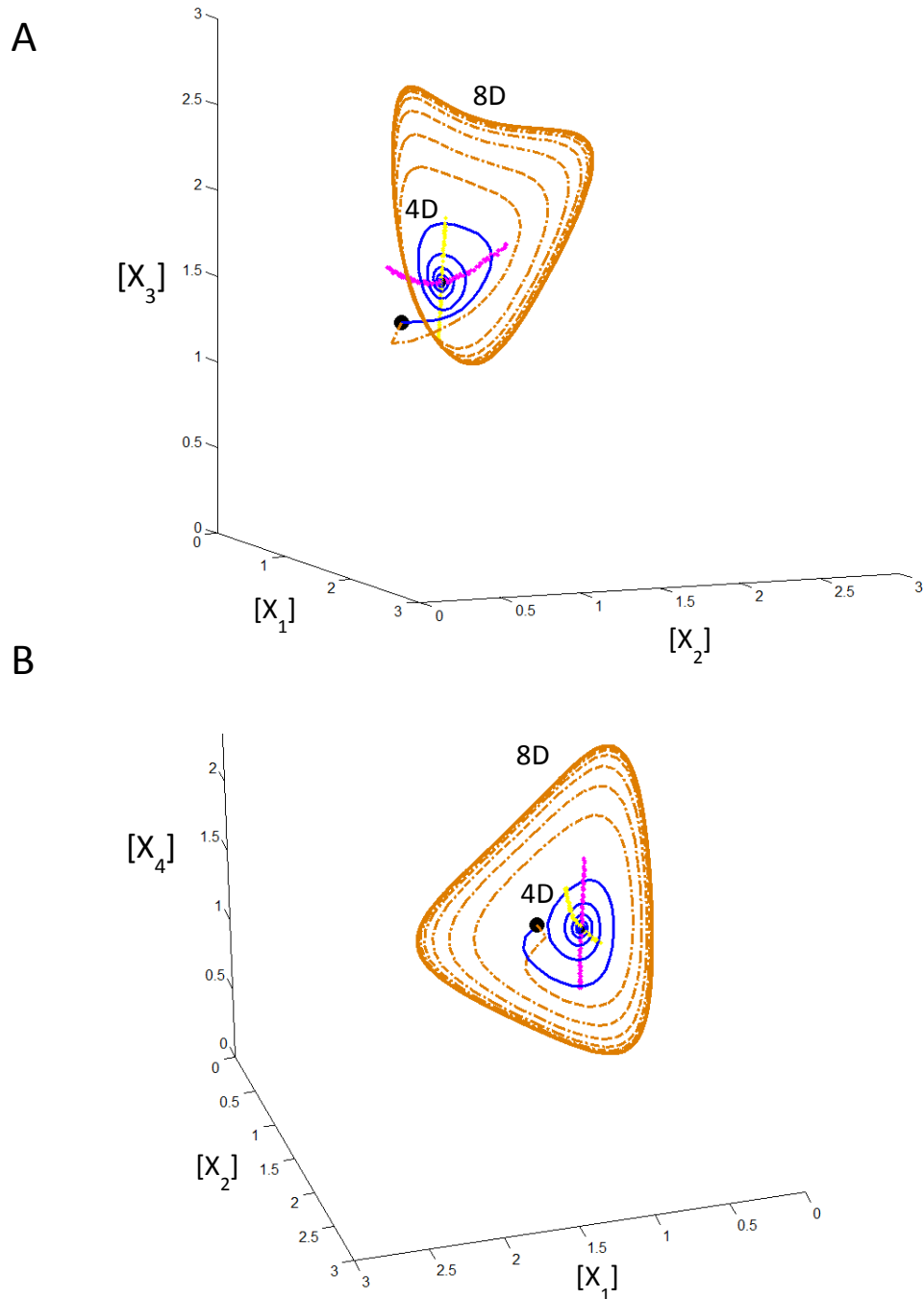


Figure S10 A and B Trajectories in the DS3 phase volume at large asymmetry, $b_{\text{common}}=10$. The 8D (finite reference time-scale separation) and 4D (infinite time-scale separation) trajectories are shown in orange and blue, respectively. Their common start point is shown by a black dot. The finite time-scale separation 8D dynamics presents a large amplitude limit-cycle. However, the infinite time-scale separation 4D dynamics is devoid of a limit cycle. Thus, the 8D trajectory reaches a dynamic attractor (stable limit cycle) but the 4D trajectory falls into a static central attractor (stable fixed point). The 123 and 234 3-variable null-surfaces are shown by colored yellow and magenta clouds of points, respectively. They intersect at the (unique) central fixed point of the dynamics (stable for 4D and unstable for 8D).